RMetS
Royal Meteorological Society

Evidence of convective transport in tropical West Pacific region during SHIVA experiment

Gisèle Krysztofiak,[1]* Valéry Catoire,[1] Paul D. Hamer,[2†] Virginie Marécal,[2] Claude Robert,[1] Andreas Engel,[3] Harald Bönisch,[3‡] Katja Grossmann,[4§] Birgit Quack,[5] Elliot Atlas[6] and Klaus Pfeilsticker[4]

[1]*LPC2E, Université Orléans − CNRS (UMR 7328), Orléans Cedex 2, France*
[2]*CNRM, Météo-France − CNRS (UMR 3589), Toulouse Cedex, France*
[3]*Department of Experimental Atmospheric Research, Institute of Atmospheric and Environmental Science, J. W. Goethe-University Frankfurt am Main, Frankfurt am Main, Germany*
[4]*Chemical Oceanography Department, Institute of Environmental Physics, Ruprecht-Karls-Universität Heidelberg, Germany*
[5]*GEOMAR Helmholtz Centre for Ocean Research Kiel, Germany*
[6]*Department of Atmospheric Sciences, Rosenstiel School for Marine and Atmospheric Sciences, Miami FL, USA*

Correspondence to:

G. Krysztofiak, Laboratoire de Physique et Chimie de l'Environnement et de l'Espace, Université d' Orléans CNRS (UMR 7328), 3A Avenue de la Recherche Scientifique, 45071 Orléans Cedex 2, France.
E-mail:
gisele.krysztofiak@cnrs-orleans.fr

[†]*Current address: NILU, PO Box 100, NO-2027 Kjeller, Norway.*
[‡]*Current address: Institute for Meteorology and Climate Research, Karlsruhe Institute of Technology, Karlsruhe, Germany.*
[§]*Current address: Joint Institute for Regional Earth System Science and Engineering (JIFRESSE), University of California Los Angeles, Los Angeles, CA 90095, USA.*

Abstract

Air masses in the convective outflows of four large convective systems near Borneo Island in Malaysia were sampled in the height range 11–13 km within the frame of the SHIVA (Stratospheric Ozone: Halogen Impacts in a Varying Atmosphere) FP7 European project in November and December 2011. Correlated enhancements of CO, CH_4 and the short-lived halogen species (CH_3I and $CHBr_3$) were detected when the aircraft crossed the anvils of the four systems. These enhancements were interpreted as the fingerprint of vertical transport from the boundary layer by the convective updraft and then horizontal advection in the outflow. For the four observations, the fraction f of air from the boundary layer ranged between 15 and 67%, showing the variability in transport efficiency depending on the dynamics of the convective system.

Keywords: convective transport; VSLS transport; *in situ* measurements; aircraft

1. Introduction

The composition of the tropical upper troposphere (UT) is affected by the efficiency of the convective transport of chemical species (Fueglistaler *et al.,* 2009). Tropical deep convection can efficiently transport surface emitted compounds from the lower troposphere into the tropical tropopause layer (TTL) altitude range (Marécal *et al.,* 2006). Since in tropical regions large emissions of halogenated very short-lived species (VSLS) coincide with deep convection, one may expect rapid transport of VSLS into the TTL. Indeed, an efficient transport of chemical tracers from polluted air masses (Bechara *et al.,* 2010) or biogenic sources from the oceans such as halogenated VSLS ($CHBr_3$, CH_2Br_2, CH_3I, etc.: Sala *et al.,* 2014; Tegtmeier *et al.,* 2013) was observed and modelled (Navarro *et al.,* 2015; Werner *et al.,* 2017).

In the last decades, several field campaigns [such as SHIVA – Stratospheric Ozone: Halogen Impacts in a Varying Atmosphere, Sala *et al.,* 2014, Fuhlbrügge *et al.,* 2016; TC4 (www.nasa.gov/mission_pages/TC4); ATTREX, Jensen *et al.* 2015] and modelling studies (Hossaini *et al.,* 2012) focused on determining the contribution of the VSLS to the bromine burden in the upper troposphere and lower stratosphere (UTLS). Observational campaigns can only address the transport into the UT on an event-like basis but they are of high interest because the convection parameterisation is a major source of uncertainty in chemistry transport models (Arteta *et al.,* 2009; Hoyle *et al.,* 2011). Previous observational studies of convective outflows at mid-latitudes (Bertram *et al.,* 2007) and in the tropics (Ray *et al.,* 2004) reported an effective transport of short-lived trace gases (Cohan *et al.,* 1999; Bechara *et al.,* 2010) by

convection from the boundary layer (BL) into the UT. These studies showed that a fraction of 20–40% of BL air was present in individual convective plumes transported rapidly to the UT.

One of the objectives of the SHIVA FP7 European project was the investigation of the atmospheric transport of VSLS from the BL into the UTLS. The campaign took place in the tropical West Pacific during the boreal winter monsoon in November and December 2011 when strong convective transport is expected to occur (e.g. Levine *et al.*, 2007; Aschmann *et al.*, 2009; Liang *et al.*, 2014). Here, we present airborne measurements for four mesoscale convective events indicating enhanced UT CO and CH_4 volume mixing ratios (vmr) that directly correlate with $CHBr_3$ and CH_3I enhancements when the aircraft passed the anvil of convective cumulus clouds. The fraction of air originating from the BL is calculated by analysis of the CO enhancements.

The SHIVA campaign and instruments are presented in Section 2. In Section 3, we discuss the meteorological conditions of the flights and the detection of convective transport and its influence on CO and CH_4 concentrations. Implications for the vertical transport for VSLS are also addressed. Section 4 concludes the study.

2. SHIVA field campaign and measurements

2.1. Measurement campaign

The SHIVA aircraft campaign took place in Malaysia between 16 November and 11 December 2011. Using the German Aerospace agency (DLR) Falcon-20 aircraft, 16 research flights were conducted from Miri (Malaysia) airport in northwestern Borneo. In the present study, the results of four flights performed on 19 November (F19NOV), 9 December 2011 (F09DEC) and two on 11 December (F11DECa and F11DECb) are described in Appendix S1 (Supporting Information). The RV *Sonne* cruise started on 15 November in Singapore, passed near the northern coast of Borneo and ended in Manila, Philippines on 29 November. Measurements on *Sonne* are used to estimate the variability of halocarbons concentration in the BL.

2.2. Experimental method

The airborne CO and CH_4 measurements were performed with the SPIRIT instrument (Catoire *et al.*, 2017), and $CHBr_3$ and CH_3I with the GHOST instrument (Sala *et al.*, 2014). Additionally, whole air samples taken in the RV Sonne were analysed for halocarbons, CO and CH_4. More detail about instrumentation is provided in Appendix S1. Relative humidity from the Falcon-20 instrument and webcam imagery from mini-DOAS instrument (Großmann, 2014) are used to study the convective condition.

3. Results and discussion

3.1. Meteorological situation of the flights

Figure 1 depicts the flight tracks together with the brightness temperatures measured by the 11-μm channel IR108 from on board the Japanese geostationary satellite MTSAT-2. Additionally, cloud height is determined based on Hamada and Nishi (2010) and Iwasaki *et al.* (2010) (not shown).

Figure 1(a) indicates the presence of a well-developed convective system around 6°N and 115.5°E during research flight F19NOV that reached a maximum height of $\sim 16 \pm 0.5$ km in altitude with an extended anvil on its west side reaching 14.5 ± 0.5 km. For F09DEC, a convective system with a smaller horizontal extent was detected at around 5.5°N and 118.5°E (Figure 1(b)). The convective part of the system reached $\sim 15.5 \pm 1$ km altitude and was embedded in stratiform clouds with maximum height $\sim 13.5 \pm 1.5$ km. In F11DECa (Figure 1(c)), a well-developed convective system was probed between 1°–2°N and 106°–107°E. The cloud top altitude for this system reached a maximum of $\sim 17 \pm 0.5$ km. The convection cell lasted throughout the day and was again probed during the back flight from Singapore to Miri in the afternoon for F11DECb (Figure 1(d)), though with a weakened strength.

3.2. Impact of deep convection on trace gases

3.2.1. CO and CH_4

Figures 2–4 show CO and CH_4 measured by the SPIRIT instrument. In all cases when the aircraft crossed convective outflows (period determined by webcam data, relative humidity and brightness temperature, see Figure 2), the mixing ratios of the measured tracers are increased. In the next section, such measurements are defined as $[X]_{UTconv}$, and the lower tracer mixing ratios observed outside of the convective system are defined as $[X]_{UT}$. CO and CH_4 are mainly emitted from anthropogenic sources in the BL. The sudden increases of $[X]_{UTconv}$, larger than the UT mixing ratios ($[X]_{UT}$), i.e. between 15 and 60 pbbv for CO and between 20 and 50 ppbv for CH_4, are thus indicative of transport of polluted air from the BL into the UT. Such enhancements of BL tracers due to convection and affecting the UT composition have also been previously reported by Bechara *et al.* (2010) and Borbon *et al.* (2012).

3.2.2. Fraction of BL air detected in the UT

CO has proven to be a particularly good tracer to study convection due to its source at the surface and tropospheric lifetime of 1–3 months (Dessler, 2002). Following Bertram *et al.* (2007), the measured tracer's mixing ratio $[X]$ is used to quantify the air fraction f originating from the BL and transported by convection, using the following equation:

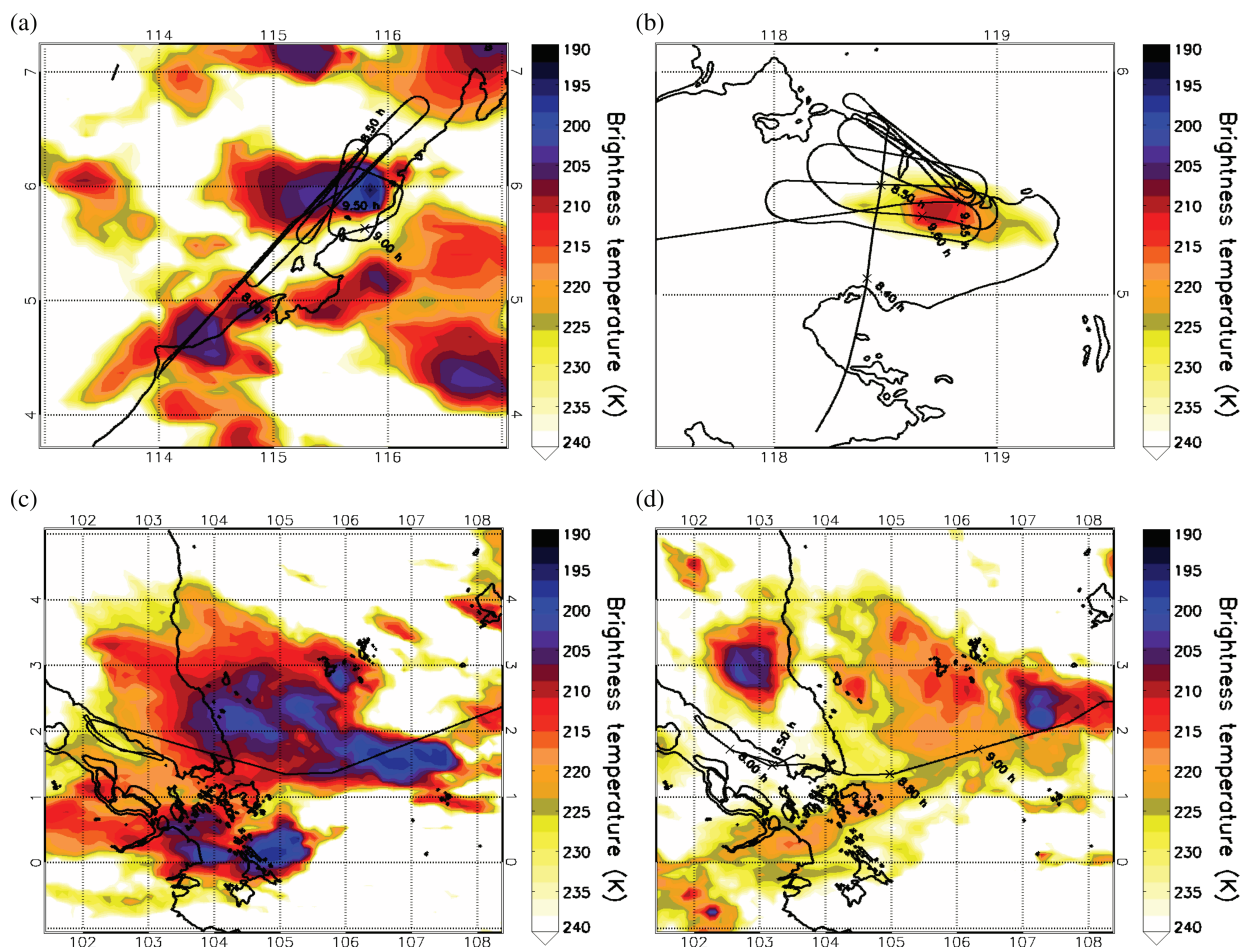$$[X]_{UTconv} = f \cdot [X]_{BL} + (1 - f) \cdot [X]_{UT} \qquad (1)$$

Figure 1. IR brightness temperature from MTSAT-2 channel IR108 (10.3–11.3 μm) for 0900 UTC on 19 November 2011 (a), 0900 UTC 9 December 2011 (b), 0400 UTC 11 December 2011 (c) and 0900 UTC on 11 December 2011 (d). The flight tracks are displayed as black lines.

where $[X]_{BL}$ represents the vmr of the tracer in the BL. For the air masses affected by convection, $[X]_{UTconv}$ is determined from the calculated means for CH_4 and CO. For F19NOV, $[X]_{BL}$ is determined from the air directly probed below the convective system during the take-off and landing since the convective system was located near Miri. For F09DEC, the surface air was directly sampled during a dive under the convective system down to 1 km altitude and for F11DECa and F11DECb, the BL measurements from RV *Sonne* are used. All relevant parameters are summarised in Table 1. In all, 18–50% of air present in the outflow of convective systems was recently transported from the BL, based on measured CO and CH_4.

3.2.3. Impact of deep convection on upper tropospheric CH_3I and $CHBr_3$

For the four studied flights, Figures 2–4 (upper panel) show GHOST-MS measurements of $CHBr_3$ and CH_3I for air affected by deep convection. As for CH_4 and CO, flight-dependent enhancements ranging from 0.3 to 0.5 pptv for CH_3I and 0.6–1.0 pptv for $CHBr_3$ are observed in the air of convective outflow.

Three areas are defined in order to calculate the BL mean concentration depending on the location of

the flight by using a combination of GHOST and RV *Sonne* measurements. For F19NOV, $[X]_{BL}$ only takes into account measurements in the region northeast of Miri, for F09DEC the region on the eastern side of Borneo and for F11DEC the region east of Singapore. Averaging over the designated areas separately removes the variability in oceanic emission sources between each region. For $CHBr_3$, it results in averaged concentrations in the range 1.8–2.7 pptv and for CH_3I in the range 0.3–0.5. The UT concentrations are calculated individually for each flight and give concentrations in the range 0.39–0.52 pptv for $CHBr_3$ and 0.21–0.25 pptv for CH_3I. According to Sala *et al.* (2014), the mean concentration of $CHBr_3$ in the UT is 0.61 ± 0.2 pptv and the mean concentration in the BL is 1.43 ± 0.53 pptv, considering data from all SHIVA flights in the tropics. However, the reported mean concentration for UT also contains the measurements affected by convection. For F19NOV, F09DEC and F11DEC, the resulting fractions f using $CHBr_3$ and CH_3I are in the range between 15 and 67%. Table 1 summarises measured and averaged mixing ratios of all gases and fractions f for $CHBr_3$ and CH_3I. Note, the calculated fractions f depend on the actual source strength at the marine boundary surface, which for $CHBr_3$ are known to strongly vary in
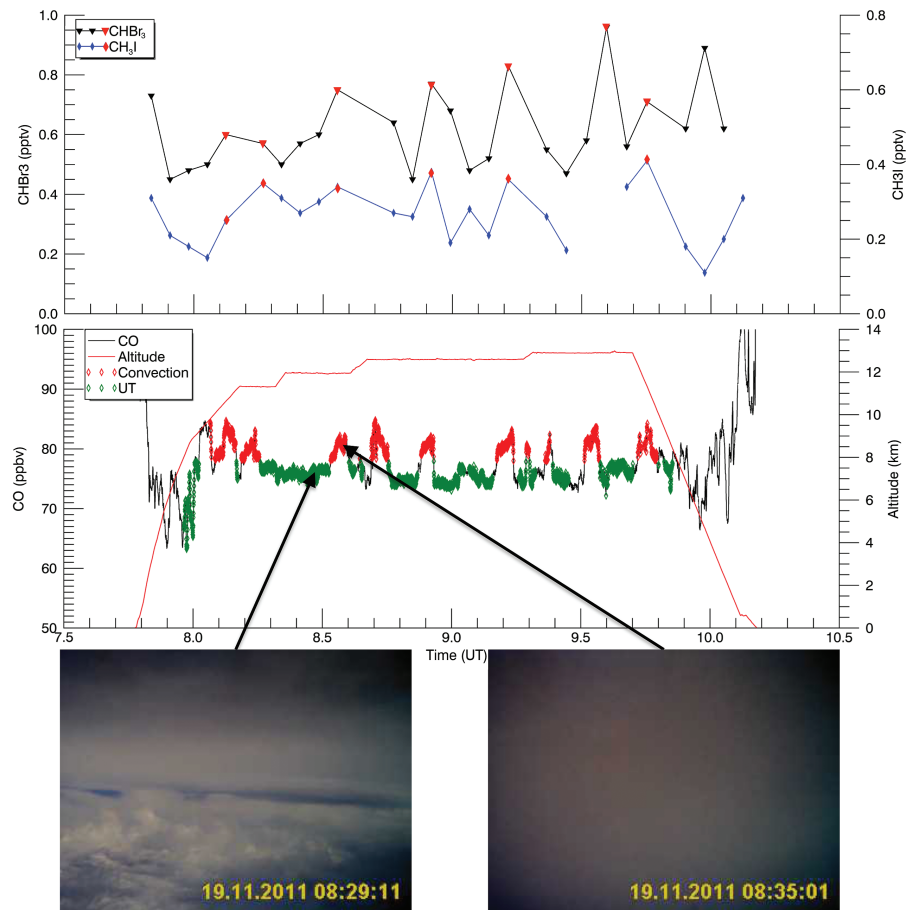
Figure 2. Measurements from aboard the Falcon-20 during SHIVA campaign during the afternoon flight on 19 November 2011. From bottom to top: mini-DOAS webcam picture, CO (in black) and altitude (in red) from SPIRIT instrument and CHBr3 (in black triangles) and CH3I (in blue lozenge) from GHOST-MS instrument. The times when the aircraft crossed the anvil cloud were determined according to the mini-DOAS webcam, the humidity data from the Falcon aircraft (showing that when the Falcon penetrating the clouds the relative humidity exceeded 100% that is indicative of supersaturated air), and the brightness temperature of the cloud area inferred from the MTSAT (for data lower than 225 K, equivalent to 13 km). In panels, these data are labelled in red. Measurements taken into account to calculate $[X]_{CONV}$ are labelled in red and for $[X]_{UT}$ in green.
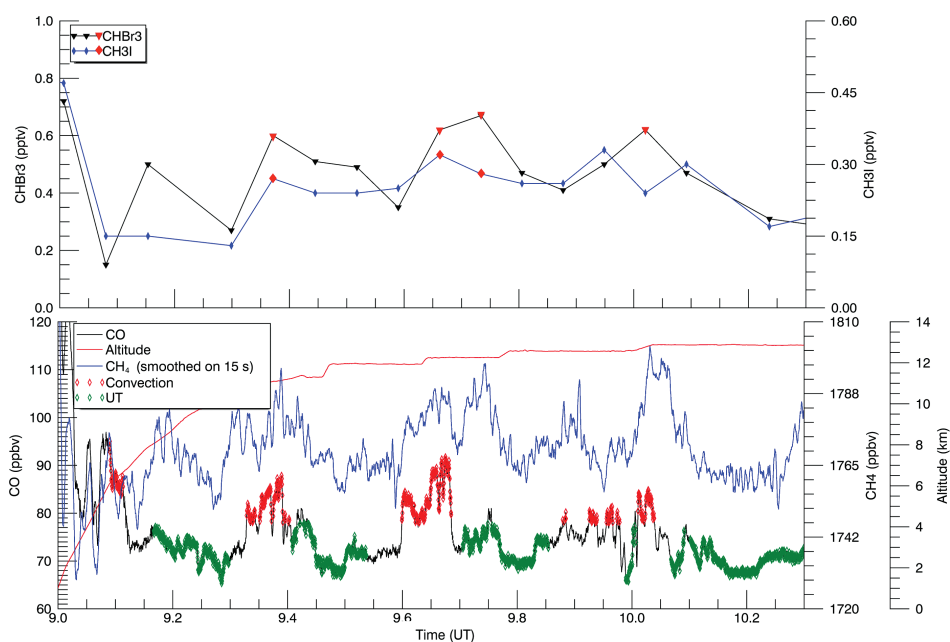

Figure 3. Same as Figure 2 but for the flight on the afternoon flight on 9 December 2011. In the bottom panel, the blue line shows the CH4 measurements of SPIRIT.
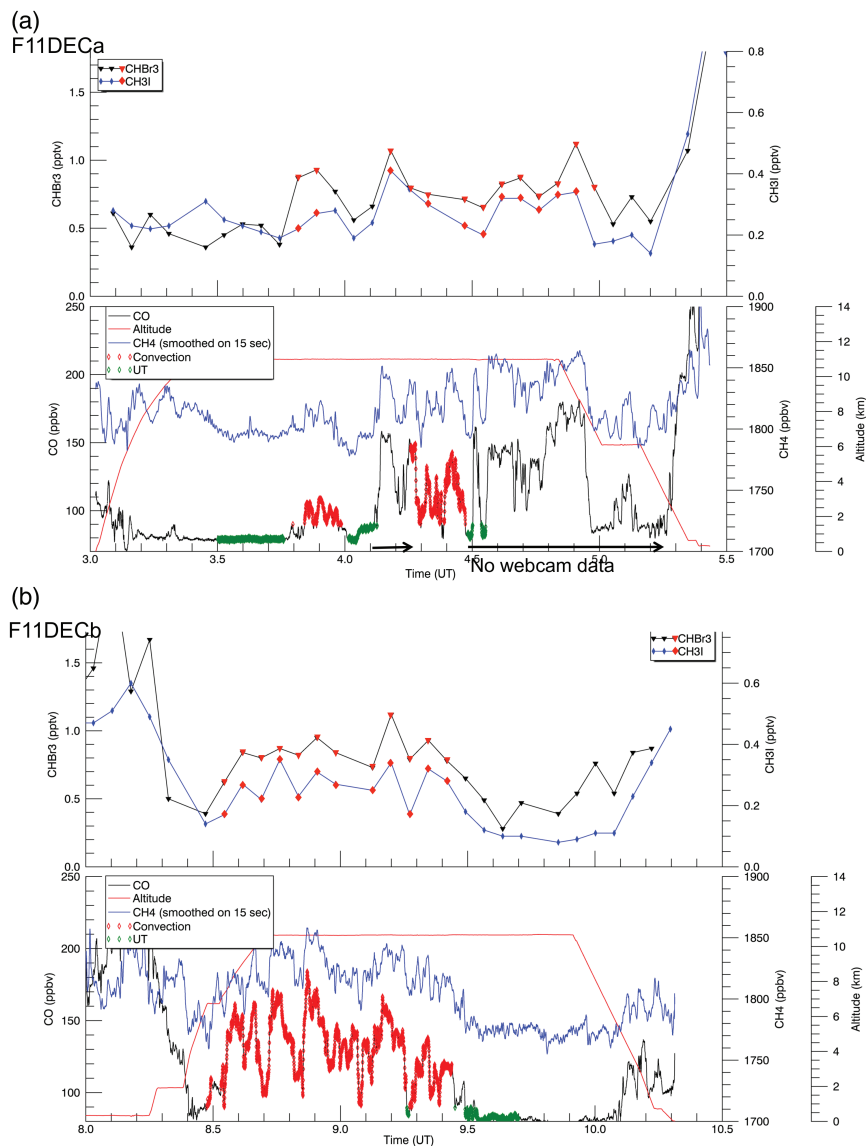
Figure 4. Same as Figures 2 and 3 but for the morning and afternoon flights on 11 December 2011.

space and time. Furthermore, since the time resolution of the CHBr$_3$ and CH$_3$I measurements is longer than for CO and CH$_4$ measurements, the different averaging time may also affect the inferred fractions f by probably biasing them low relative to f calculated from other trace gases.

3.2.4. Comparison with previous studies

Considering all species from all flights, a mean fraction of $29 \pm 25\%$ is obtained (mean of the fractions f with standard deviations $\sigma < 0.4$). Table 1 compares our inferred fractions f with those found in the literature. The inferred mean fraction f derived from CO and CH$_4$ (18%–50%) is in reasonable agreement with the fraction f inferred by Bertram *et al.* (2007), Ray *et al.* (2004), Lopez *et al.* (2006) and Bechara *et al.* (2010) given the range uncertainties. Like in our study, these authors used CO and CH$_4$ measurements among other tracers to calculate the fractions f. The fractions of Cohan *et al.* (1999) and Barth *et al.* (2016) using VSLS

CH$_3$I, CH$_3$O$_2$H, CHBr$_3$ and VOCs are in agreement with our results (15–67%) derived from CHBr$_3$ and CH$_3$I.

Also, from the previous studies related to SHIVA project, Großmann (2014) inferred a fraction of 19% for the short-lived species HCHO measured during F19NOV using a mini-DOAS instrument (Stutz *et al.*, 2017) and Fuhlbrügge *et al.* (2016) calculated similar contributions of marine BL air to the free troposphere (30–50%) up to 13 km height for the whole SHIVA-campaign with a trajectory model, again in agreement with the results of the present study.

4. Conclusions

Within the frame of the SHIVA project, air of the anvil from mesoscale large convective systems was sampled at altitudes around 11–13 km near Borneo (6.0°N–115.5°E and 5.5°N–118.5°E) and Singapore (1°N–106°E) on 19 November, 9 and 11 December

Table 1. SPIRIT measured mean mixing ratios of CO, CH$_4$, CHBr$_3$ and CH$_3$I for the boundary layer ([X]$_{BL}$), upper troposphere ([X]$_{UT}$) and convective air masses ([X]$_{UTconv}$) during the flights on 19 November 2011, 9 December 2011 and 11 December 2011.

			[X]$_{BL}$[a]	[X]$_{UT}$[a]	[X]$_{UTconv}$[a]	fraction f[b]	Comment
This study	F19NOVb	CO[c]	95 ± 12	76 ± 2	81 ± 1	0.26 ± 0.21	Borneo region (6°N–117°E)
		CHBr$_3$[d]	1.82 ± 0.86	0.51 ± 0.04	0.73 ± 0.12	0.17 ± 0.15	
		CH$_3$I[d]	0.43 ± 0.17	0.24 ± 0.06	0.35 ± 0.05	0.59 ± 0.70	
	F09DECb	CO[c]	129 ± 9	73 ± 3	83 ± 3	0.18 ± 0.08	
		CH$_4$[c]	1801 ± 25	1771 ± 11	1782 ± 10	0.37 ± 0.60	
		CHBr$_3$[d]	2.32 ± 1.66	0.39 ± 0.12	0.69 ± 0.03	0.16 ± 0.15	
		CH$_3$I[d]	0.52 ± 0.54	0.22 ± 0.06	0.28 ± 0.03	0.20 ± 0.43	
	F11DECa	CO[c]	179	81 ± 3	109 ± 15	0.29 ± 0.16	
		CH$_4$[c]	1868	1794 ± 6	1817 ± 13	0.31 ± 0.20	
		CHBr$_3$[d]	2.71 ± 0.89	0.50 ± 0.1	0.84 ± 0.13	0.15 ± 0.10	
		CH$_3$I[d]	0.32 ± 0.02	0.23 ± 0.04	0.29 ± 0.07	0.67 ± 0.96	
	F11DECb	CO[c]	179	83 ± 2	131 ± 20	0.50 ± 0.21	
		CH$_4$[c]	1868	1776 ± 8	1822 ± 16	0.50 ± 0.20	
		CHBr$_3$[d]	2.71 ± 0.89	0.51 ± 0.16	0.84 ± 0.12	0.15 ± 0.11	
		CH$_3$I[d]	0.32 ± 0.02	0.21 ± 0.03	0.27 ± 0.06	0.55 ± 0.35	
	Mean					0.29 ± 0.25[e]	
Cohan *et al.* (1999)						0.36−0.68	South Pacific (60°S−10°N)
Ray *et al.* (2004)						0.20−0.45	Mexican Gulf (20°N)
Lopez *et al.* (2006)						0.2−0.4	Subtropical, Florida
Bertram *et al.* (2007)						0.17 ± 0.08	Eastern United States and Canada
Bechara *et al.* (2010)						0.40 ± 0.15	West Africa
Großmann (2014)						0.19	Borneo region
Derived from Barth *et al.* (2016)						0.27−0.58	Oklahoma and northeast Colorado

These inferred vmr are used in the calculation of the fraction f of air coming from the boundary layer detected in the convective air mass. The mean fraction f found is compared with other studies.

[a]Uncertainties are 1σ on the mean.
[b]Uncertainties include propagation error of the standard deviation of individual values.
[c]Volume mixing ratio in ppbv.
[d]Volume mixing ratio in pptv.
[e]Mean of the fraction f with standard deviations $\sigma < 0.4$.

2011, respectively. Correlated measurements of CO, CH$_4$, CHBr$_3$ and CH$_3$I were interpreted with respect to the strength of air mass transported from the BL to the UT by convective systems. The fraction f of BL air contained in the fresh convective outflow was calculated to range between 18 and 50% based on measured CO and CH$_4$. Correlative measurements of CHBr$_3$ and CH$_3$I indicated a fraction between 15 and 67%. The inferred range of f indicates the variability in mixing due to air mass entrainment into the convective system, but also points to limitations in the method due to its dependence on the variability of the tracer's source strength and lifetime of the species

To go a step further, modelling or measurements from higher flying platforms, such as recently performed from the Global Hawk in the NASA ATTREX project over the Pacific, may provide estimates of the transport of halogenated VSLS due to deep convection reaching the TTL (e.g. Werner *et al.*, 2017).

Acknowledgements

Supporting information

The following supporting information is available:

Appendix S1. Campaign and instruments description.

References

Arteta J, Marécal V, Rivière ED. 2009. Regional modelling of tracer transport by tropical convection. Part 1: sensitivity to convection parameterization. *Atmospheric Chemistry and Physics* **9**: 7081–7100.

Aschmann J, Sinnhuber B-M, Atlas EL, Schauffler SM. 2009. Modeling the transport of very short-lived substances into the tropical upper troposphere and lower stratosphere. *Atmospheric Chemistry and Physics* **9**: 9237–9247. https://doi.org/10.5194/acp-9-9237-2009.

Barth MC, Bela MM, Fried A, Wennberg PO, Crounse JD, St. Clair JM, Blake NJ, Blake DR, Homeyer CR, Brune WH, Zhang L, Mao J, Ren X, Ryerson TB, Pollack IB, Peischl J, Cohen RC, Nault BA, Huey LG, Liu X, Cantrell CA. 2016. Convective transport of peroxides by thunderstorms observed over the Central U.S. during DC3. *Journal of Geophysical Research – Atmospheres* **121**: 4272–4295. https://doi.org/10.1002/2015JD024570.

Bechara J, Borbon A, Jambert C, Colomb A, Perros PE. 2010. Evidence of the impact of deep convection on reactive volatile organic compounds in the upper tropical troposphere during the AMMA experiment in West Africa. *Atmospheric Chemistry and Physics* **10**: 10321–10334. https://doi.org/10.5194/acp-10-10321-2010.

Bertram TH, Perring AE, Wooldridge PJ, Crounse JD, Kwan AJ, Wennberg PO, Scheuer E, Dibb J, Avery M, Sachse G, Vay SA, Crawford JH, McNaughton CS, Clarke A, Pickering KE, Fuelberg H, Huey G, Blake DR, Singh HB, Hall SR, Shetter RE, Fried A, Heikes BG, Cohen RC. 2007. Direct measurements of the convective recycling of the upper troposphere. *Science* **315**: 816–820.

Borbon A, Ruiz M, Bechara J, Aumont B, Chong M, Huntrieser H, Mari C, Reeves CE, Scialom G, Hamburger T, Stark H, Afif C, Jambert C, Mills G, Schlager H, Perros PE. 2012. Transport and chemistry of formaldehyde by mesoscale convective systems in West Africa during AMMA 2006. *Journal of Geophysical Research* **117**: D12301. https://doi.org/10.1029/2011JD017121.

Catoire V, Robert C, Chartier M, Jacquet P, Guimbaud C, Krysztofiak G. 2017. The SPIRIT airborne instrument: a three-channel infrared absorption spectrometer with quantum cascade lasers for in-situ atmospheric trace-gas measurements. *Applied Physics B* **123**: 244. https://doi.org/10.1007/s00340-017-6820-x.

Cohan DS, Schultz MG, Jacob DJ, Heikes BG, Blake DR. 1999. Convective injection and photochemical decay of peroxides in the tropical upper troposphere: methyl iodide as a tracer of marine convection. *Journal of Geophysical Research* **104**: 5717–5724.

Dessler AE. 2002. The effect of deep, tropical convection on the tropical tropopause layer. *Journal of Geophysical Research* **107**: 2156–2202. https://doi.org/10.1029/2001JD000511.

Fueglistaler S, Dessler AE, Dunkerton TJ, Folkins I, Fu Q, Mote PW. 2009. Tropical tropopause layer. *Reviews of Geophysics* **47**: RG1004. https://doi.org/10.1029/2008RG000267.

Fuhlbrügge S, Quack B, Tegtmeier S, Atlas E, Hepach H, Shi Q, Raimund S, Krüger K. 2016. The contribution of oceanic halocarbons to marine and free tropospheric air over the tropical West Pacific. *Atmospheric Chemistry and Physics* **16**: 7569–7585. https://doi.org/10.5194/acp-16-7569-2016.

Großmann K. 2014. *Aircraft-Borne DOAS Limb Observations of UV/Visible Absorbing Trace Gas Species over Borneo: Implications for the Photochemistry of Iodine, Volatile Organic Oxide Degradation, and Lightning-Produced Radicals*. University of Heidelberg: Heidelberg.

Hamada A, Nishi N. 2010. Development of a cloud-top height estimation method by geostationary satellite split-window measurements trained with CloudSat data. *Journal of Applied Meteorology and Climatology* **49**: 2035–2049.

Hossaini R, Chipperfield MP, Feng W, Breider TJ, Atlas E, Montzka SA, Miller BR, Moore F, Elkins J. 2012. The contribution of natural and anthropogenic very short-lived species to stratospheric bromine. *Atmospheric Chemistry and Physics* **12**: 371–380. https://doi.org/10.5194/acp-12-371-2012.

Hoyle CR, Marécal V, Russo MR, Allen G, Arteta J, Chemel C, Chipperfield MP, D'Amato F, Dessens O, Feng W, Hamilton JF, Harris NR, Hosking JS, Lewis AC, Morgenstern O, Peter T, Pyle JA, Reddmann T, Richards NAD, Telford PJ, Tian W, Viciani S, Volz-Thomas A, Wild O, Yang X, Zeng G. 2011. Representation of tropical deep convection in atmospheric models. Part 2: tracer transport. *Atmospheric Chemistry and Physics* **11**: 8103–8131.

Iwasaki S, Shibata T, Nakamoto J, Okamoto H, Ishimoto H, Kubota H. 2010. Characteristics of deep convection measured by using the A-train constellation. *Journal of Geophysical Research* **115**: D06207. https://doi.org/10.1029/2009JD013000.

Jensen EJ, Pfister L, Jordan DE, Bui TV, Ueyama R, Singh HB, Thornberry T, Rollins AW, Gao R-S, Fahey DW, Rosenlof KH, Elkins JW, Diskin GS, Di-Gangi JP, Lawson RP, Woods S, Atlas EL, Rodriguez MAN, Wofsy SC, Pittman J, Bardeen CG, Toon OB, Kindel BC, Newman PA, McGill MJ, Hlavka DL, Lait LR, Schoeberl MR, Bergman JW, Selkirk HB, Alexander MJ, Kim J-E, Lim BH, Stutz J, Pfeilsticker K. 2015. The NASA Airborne Tropical TRopopause EXperiment (ATTREX): high-altitude aircraft measurements in the tropical Western Pacific. *Bulletin of the American Meteorological Society* **12/2015**: 129–144. https://doi.org/10.1175/BAMS-D-14-00263.1.

Levine JG, Braesicke P, Harris NRP, Savage NH, Pyle JA. 2007. Pathways and timescales for troposphere-to-stratosphere transport via the tropical tropopause layer and their relevance for very short lived substances. *Journal of Geophysical Research* **112**: D04308. https://doi.org/10.1029/2005JD006940.

Liang Q, Atlas E, Blake D, Dorf M, Pfeilsticker K, Schauffler S. 2014. Convective transport of very short lived bromo-carbons to the stratosphere. *Atmospheric Chemistry and Physics* **14**: 5781–5792. https://doi.org/10.5194/acp-14-5781-2014.

Lopez JP, Fridlind AM, Jost H-J, Loewenstein M, Ackerman AS, Campos TL, Weinstock EM, Sayres DS, Smith JB, Pittman JV, Hallar AG, Avallone LM, Davis SM, Herman RL. 2006. CO signatures in subtropical convective clouds and anvils during CRYSTAL-FACE: an analysis of convective transport and entrainment using observations and a cloud-resolving model. *Journal of Geophysical Research* **111**: D09305. https://doi.org/10.1029/2005JD006104.

Marécal V, Rivière ED, Held G, Cautenet S, Freitas S. 2006. Modelling study of the impact of deep convection on the UTLS air composition. Part I: analysis of ozone precursors. *Atmospheric Chemistry and Physics* **6**: 1567–1584.

Navarro MA, Atlas EL, Saiz-Lopez A, Rodriguez-Lloveras X, Kinnison DE, Lamarque J-F, Tilmes S, Filus M, Harris NRP, Meneguz E, Ashfold MJ, Manning AJ, Cuevas CA, Schauffler SM, Donets V. 2015. Airborne measurements of organic bromine compounds in the Pacific tropical tropopause layer. *Proceedings of the National Academy of Sciences of the United States of America* **112**: 13789–13793. https://doi.org/10.1073/pnas.1511463112.

Ray EA, Rosenlof KH, Richard EC, Hudson PK, Cziczo DJ, Loewenstein M, Jost H-J, Lopez J, Ridley B, Weinheimer A, Montzka D, Knapp D, Wofsy SC, Daube BC, Gerbig C, Xueref I, and. Herman R. L. 2004. Evidence of the effect of summertime midlatitude convection on the subtropical lower stratosphere from CRYSTAL-FACE tracer measurements. *Journal of Geophysical Research* **109**: D18304. https://doi.org/10.1029/2004JD004655.

Sala S, Bönisch H, Keber T, Oram DE, Mills G, Engel A. 2014. Deriving an atmospheric budget of total organic bromine using airborne in situ measurements from the western Pacific area during SHIVA. *Atmospheric Chemistry and Physics* **14**: 6903–6923. https://doi.org/10.5194/acp-14-6903-2014.

Stutz J, Werner B, Spolaor M, Scalone L, Festa J, Tsai C, Cheung R, Colosimo SF, Tricoli U, Raecke R, Hossaini R, Chipperfield MP, Feng W, Gao R-S, Hintsa EJ, Elkins JW, Moore FL, Daube B, Pittman J, Wofsy S, Pfeilsticker K. 2017. A new differential optical absorption spectroscopy instrument to study atmospheric chemistry from a high-altitude unmanned aircraft. *Atmospheric Measurement Techniques* **10**: 1017–1042. https://doi.org/10.5194/amt-10-1017-2017.

Tegtmeier S, Krüger K, Quack B, Atlas E, Blake DR, Boenisch H, Engel A, Hepach H, Hossaini R, Navarro MA, Raimund S, Sala S, Shi Q, Ziska F. 2013. The contribution of oceanic methyl iodide to stratospheric iodine. *Atmospheric Chemistry and Physics* **13**: 11869–11886. https://doi.org/10.5194/acp-13-11869-2013.

Werner B, Stutz J, Spolaor M, Scalone L, Raecke R, Festa J, Colosimo SF, Cheung R, Tsai C, Hossaini R, Chipperfield MP, Taverna GS, Feng W, Elkins JW, Fahey DW, Gao R-S, Hintsa EJ, Thornberry TD, Moore FL, Navarro MA, Atlas E, Daube BC, Pittman J, Wofsy S, Pfeilsticker K. 2017. Probing the subtropical lowermost stratosphere and the tropical upper troposphere and tropopause layer for inorganic bromine. *Atmospheric Chemistry and Physics* **17**: 1161–1186. https://doi.org/10.5194/acp-17-1161-2017.